Multi-source 3D point clouds fusion for potential rock mass hazard evaluation in high-steep rock slopes

Wei Yuan [1], Changqing Liu [1,2], Tianyi Wang [2], Bruno Adriano [1], Han Bao [2], Ryosuke Shibasaki [3], Shunichi Koshimura[1]

[1] International Research Institute of Disaster Science, Tohoku University, Sendai, Japan – (wei.yuan, changqing.liu.d8, bruno.adriano, koshimura) @tohoku.ac.jp
[2] School of Highway, Chang'an University, Xi'an, China – (17803867672, baohangeo) @163.com
[3] Department of Engineering, Reitaku University, Chiba, Japan – shiba@csis.u-tokyo.ac.jp

Keywords: Rock slope, Hazardous rock mass, Intelligent evaluation, 3D point clouds, TLS, UAV.

Abstract

Accurate characterization and evaluation of hazardous rockmass sources prove essential for rockfall risk mitigation. Structural properties of rock masses play a decisive role in evaluating these risks. This study presents an integrated approach that combines Terrestrial Laser Scanning (TLS) and Unmanned Aerial Vehicle (UAV) photogrammetry to address data limitations in complex terrain. The practical validation was carried out on the basis of a case study on a high and steep rock slope. The results demonstrate that the fusion of TLS-UAV multi-source data enhances spatial coverage and point cloud density by 19%, enabling comprehensive slope modeling and improving multi-angle structural characterization of target rock masses. An approach integrating multiple algorithms enables the automatic identification of rock joints from multi-source 3D point clouds, achieving high recognition accuracy. And the key geometric and mechanical parameters were extracted and analyzed to quantify joint properties. Furthermore, a novel rock hazard index (*RHI*) is proposed, which takes into account joint geometric features, joint mechanical features, and slope quality grade to assess risk levels across slope domains. The proposed framework provides an efficient solution for joint-controlled hazardous rockmass assessment, offering theoretical insights and practical applications for infrastructure-related geohazard prevention. This study contributes to enhancing risk assessment methodologies for high and steep slope environments.

1. Introduction

During the construction and operation of transportation corridors in mountainous areas, the steep rock slopes along the route are susceptible to instability, which often triggers geological hazards such as rockfalls, landslides, and debris flows (Lan et al., 2024; Liu et al., 2024b). Among these, the instability and collapse of joint-controlled rock masses caused by multi-scale discontinuities represent a predominant threat. Severe disasters caused by the instability of hazardous rock masses have led to significant transportation disruptions worldwide (Mirhadi and Macciotta, 2023; Li et al., 2024). Hence, establishing a reliable and efficient method for detecting hazardous rock masses and evaluating potential risk sources is crucial.

Field investigations have revealed that hazardous rock masses are extensively distributed along slopes, primarily resulting from the complex interplay of multiple intersecting joints (Fig. 1). These geological hazards not only have the potential to severely damage transportation infrastructure but also pose direct threats to traffic safety, human lives, and property (Lan et al. 2022; Zhao et al. 2023). Advancements in remote sensing technologies, particularly Terrestrial Laser Scanning (TLS) and Unmanned Aerial Vehicles (UAVs), offer new avenues for acquiring detailed information on hazardous rock masses and identifying potential hazard sources (Yuan et al. 2023; 2024). TLS has gained significant attention for its ability to generate high-precision point cloud data, enabling the accurate capture of slope details and providing valuable spatial information. This technology exhibits strong resistance to interference from varying lighting conditions and vegetation coverage. However, TLS often suffers from line-of-sight occlusion in complex terrains, leading to data gaps (Battulwar et al., 2021). Additionally, setting up TLS scanning stations in steep terrains is challenging, and the equipment is cumbersome to transport. UAVs, with their high mobility and extensive coverage, can efficiently access hard-to-reach areas and acquire large-scale topographic data. When combined with real-time kinematic technology, UAVs are particularly suitable for surveying open, high and steep slopes and conducting continuous measurements. However, UAV data quality is highly susceptible to environmental factors such as weather and vegetation (Loiotine et al., 2021). The accuracy of UAV imagery and models relies heavily on the distribution and quantity of ground control points (GCPs), and establishing GCPs in complex terrains is both labor-intensive and time-consuming (Martínez et al., 2018). Both TLS and UAV technologies have distinct advantages in surveying slopes within mountainous canyon terrains, yet a single method alone is insufficient to achieve comprehensive measurement coverage in complex topographies (Ge et al., 2023). Therefore, integrating multi-source remote sensing technologies in a complementary manner can provide a more comprehensive and reliable foundation for the digital modeling of high and steep slopes and disaster risk assessment.

Figure 1. Typical examples of hazardous rock masses and rockfalls triggered by joint formations surrounding the studied rock slope.

To address these issues, this study proposes a novel method for evaluating rockmass hazard sources in rock slopes by

integrating TLS and UAV technologies. The analysis focuses on the rock slope around the Sichuan Yanjiang Expressway, a major engineering project in China (Figure 2). This study systematically evaluates rockmass hazard sources by identifying and analyzing the geometric characteristics and structural properties of rock mass structures, which derived from multi-source 3D point clouds created. This approach provides a solid foundation for accurately assessing the stability of rock slopes and offers a means to evaluate both the risk levels and spatial heterogeneity of hazard sources. As a result, this research helps mitigate the risk of instability and collapse in high and steep rock slopes.

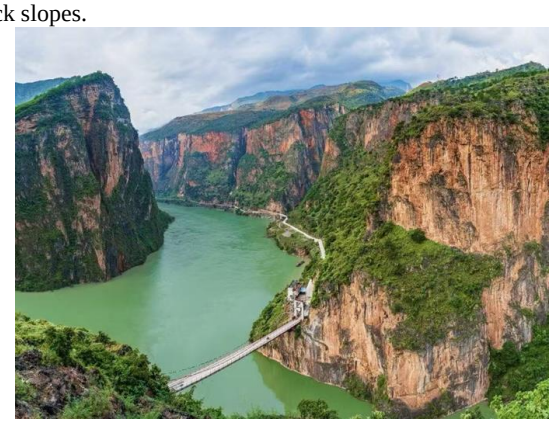

Figure 2. The rock slope and the Sichuan Yanjiang Expressway in China.

2. Related Works

Researchers have attempted to conduct comparative analysis and fusion studies of multi-source technologies to compensate for the deficiencies of individual technologies in terms of accuracy, coverage, and adaptability to complex environments (Liu et al., 2025). For example, Shan et al. (2014) improved the accuracy of ground-based multi-view 3D reconstruction (MVS) and aerial image modeling by introducing an innovative viewpoint change matching method. Zang et al. (2019) proposed a method based on patch continuity, which extracts regional features through point cloud clustering and constructs a volume model to register high-precision TLS and UAV point clouds in complex mountainous terrain. Mao et al. (2021) achieved effective data fusion by combining low-precision UAV point clouds with high-precision TLS point clouds and applying the ICP algorithm. These studies demonstrate that combining the high-precision characteristics of TLS with the wide-area coverage capabilities of UAVs can enhance data integrity and accuracy, effectively addressing the challenges posed by complex environments.

To address the challenges of multi-source point cloud registration, researchers are exploring ways to effectively compensate for data discrepancies while improving registration accuracy and efficiency. Deep learning has demonstrated significant potential in point cloud processing, including registration tasks (Huang et al., 2021). However, its practical application is often limited by the difficulty of obtaining high-quality training datasets (Yuan et al., 2023). Building a sufficiently large and diverse dataset requires extensive manual annotation and verification, making the process both time-consuming and labor-intensive (An et al., 2024). Furthermore, deep learning models trained on specific datasets often fail to generalize to complex real-world scenarios, especially for high and steep rock slopes with diverse geological conditions. In contrast, traditional methods, such as the Iterative Closest Point (ICP) algorithm, provide a more practical and adaptable solution (Besl and McKay, 1992; Marani et al., 2016). These methods do not depend on pre-trained models and can be directly applied to different datasets without extensive training. ICP offers a plug-and-play capability, enabling effective registration of TLS and UAV point clouds in diverse conditions (Mao et al., 2021). By utilizing geometric and spatial relationships within the point cloud, traditional algorithms ensure reliable alignment, making them ideal for scenarios.

On this basis, researchers have proposed various methods for identifying rock joints from 3D point clouds. One approach utilizes remote sensing technologies to capture point cloud data, which is subsequently transformed into irregular triangular mesh models for joint detection through plane fitting (Battulwar et al., 2021). Parallel to this approach, alternative methods have emerged that process joint information directly from raw point cloud data (Xu et al., 2022). These methods leverage the three-dimensional coordinate information to characterize the spatial geometry of joints, employing advanced computational algorithms to achieve automated identification. Several integrated algorithms and software solutions have been developed to enhance practical applications (Riquelme et al., 2014). Among these, Discontinuity Set Extractor has undergone continuous refinement and validation, with its effectiveness in joint characterization well-documented in recent studies (Herrero et al., 2022). Furthermore, the integration of geometric analysis theory has enabled sophisticated interpretation and statistical evaluation of key joint parameters, including set quantity, spatial orientation, persistence characteristics, spacing intervals, and surface roughness (Kong et al., 2021; Li et al., 2022). The non-contact and rapid acquisition of geometric and mechanical parameters of joints is essential for evaluating rock mass hazard sources.

3. Methods

This study introduces a novel approach for assessing rockmass hazard sources in high and steep rock slopes by leveraging TLS-UAV integrated technologies. The methodology comprises three key steps: (1) data acquisition and processing of high and steep rock slopes using combined TLS-UAV techniques, (2) creation of a multi-source 3D point cloud model through the ICP algorithm, and (3) development of an evaluation index for rockmass hazard sources that incorporates joint geometric characteristics, joint mechanical properties, and slope quality grade. The workflow is visually summarized in Figure 3, with comprehensive implementation details discussed in subsequent sections.

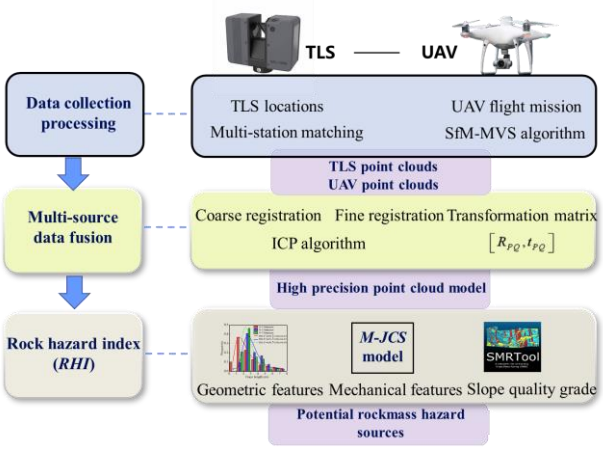

Figure 3. Multi-source 3D point clouds fusion for potential rockmass hazard evaluation in rock slopes based on TLS-UAV technologies.

4. Results and analysis

4.1 Data acquisition and processing

The SOUTH SPL-1500 is a pulse-based TLS system capable of achieving a resolution of 3 mm at a distance of 100 m. With its high-speed data acquisition capability, capturing up to 2 million points per second, this system is particularly well-suited for fast and accurate measurements as well as the creation of detailed 3D models of various targets (Liu et al., 2025). Furthermore, the system includes a high-resolution integrated camera, which enables the precise application of RGB color values to the point clouds, enhancing the visual representation of the scanned data. The key technical specifications of the TLS system are detailed in Table 1. And the DJI Phantom 4 RTK, utilized in this study, is a UAV equipped with a high-precision network Real Time Kinematic module, enabling real-time positioning accuracy at the centimeter level. The primary technical specifications of this UAV system are outlined in Table 1. To accurately capture the intricate geometry of the target slope and ensure comprehensive spatial coverage, a combination of oblique and nap-of-the-object photogrammetry was conducted under manual control. The image overlap rate in both forward and side directions was maintained at over 70%. Additional flights were necessary to capture detailed images of structurally complex rock outcrops of interest. During these flights, the UAV's built-in position and orientation system (POS) recorded essential data.

Instrument	Items	Values
UAV	Weight	1391 g
	Flight height	500 m
	Max flight time	30 min
	Image dimensions	5472*3648 pixels
	Focal length	8.8-24 mm
	Post-processing software	Metashape
TLS	Max service time	4 hours
	Ranging method	Pulse-type
	Max scanning distance	1500 m
	Distance resolution	3 mm@100m
	Angular resolution	0.001°
	Post-processing software	SouthLidar Pro

Table 1 Technical parameters of SOUTH SPL-1500 terrestrial laser scanning and DJI Phantom4 RTK unmanned aerial vehicle

To effectively capture the 3D point cloud data of the target slope, the TLS system was positioned at several locations. Once the on-site scanning process was completed, the collected point cloud data from these multiple positions were initially aligned manually using the "Station Measurement" feature in the SouthLidar Pro 2.0 software. This was followed by a more precise alignment using the multi-station adjustment technique. The UAV captured multiple images of the slope at different times, with varying capture settings, and with a specified overlap rate. These images can be processed using the Structure-from-Motion (SfM) algorithm to reconstruct a detailed 3D model of the target object. Several software solutions including Agisoft Metashape have been developed to facilitate the generation of 3D point cloud models through the SfM algorithm. The processing steps are as follows: uploading the captured images to the software and import relevant flight information; matching key features across different images using the scale-invariant feature transform (SIFT) algorithm; generating a sparse point cloud via the SfM algorithm; and constructing an enhanced dense point cloud using the multi-view stereo (MVS) algorithm. Figure 4 shows the point clouds of the high and steep rock slope acquired by TLS and UAV, respectively.

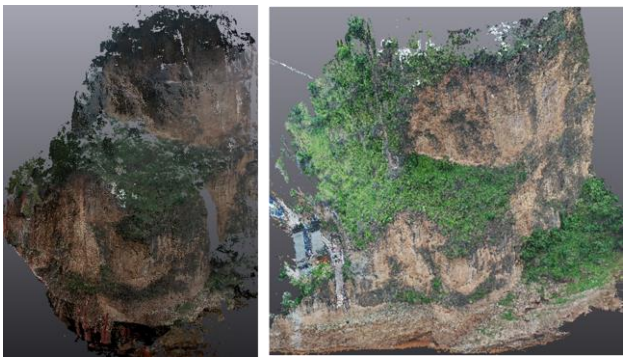

Figure 4. 3D point cloud generated from TLS (left figure), UAV images (right figure).

4.2 Multi-source data fusion

In this study, the Iterative Closest Point (ICP) algorithm was utilized for the fusion and registration of multi-source point cloud data, with the objective of enhancing the quantitative and qualitative accuracy of the point cloud model.

The ICP procedure establishes spatial correspondence between point clouds through nearest-neighbor association, iteratively refining rigid transformation parameters (rotation R, translation t) until convergence criteria are satisfied. The optimization workflow comprises four core phases:

(1) Correspondence matching

The TLS-based point cloud serves as the source $X = \{x_i\}_{i=1}^{N}$ and the UAV-based point cloud acts as the target $Y = \{y_j\}_{j=1}^{M}$. For each point x_i in the source point cloud, the closest point y_j in the target point cloud is identified based on a chosen distance metric, typically Euclidean distance:

$$y_i = arg\min_{y_j \in Y} \| x_i - y_j \| \quad (1)$$

(2) Rigid transformation estimation

Solve the procrustes problem via singular value decomposition (SVD) to determine optimal spatial alignment parameters::

$$arg\frac{\min}{R,t}\sum_{i=1}^{K} \| Rx_i + t - y_i \|_2^2 \quad (2)$$

where K is the number of valid correspondences.

(3) Apply registration

Based on the rigid transformation parameters obtained in Step 2, the new spatial coordinates of the reference point set can be derived.

$$x_i^{'} = Rx_i + t \quad (3)$$

(4) Check Convergence

The alignment error, typically measured using the Root Mean Square Error (RMSE), is evaluated:

$$E = \frac{1}{N}\sum_{i=1}^{N} \| \mathrm{x}_i^{'} - \mathrm{y}_i \|^2 \quad (4)$$

The algorithm concludes when any of the following conditions are fulfilled: The alignment error E falls below a designated threshold. The transformation change between successive iterations is minimal. The iteration count reaches its predefined limit. If none of these conditions are met, the algorithm continues iterating from Step 2 until it converges.

The integration of TLS and UAV data resulted in a heterogeneous data model comprising approximately 93.5 million points, generated using ICP registration (Figure 5). This model significantly expanded the slope coverage area compared to the TLS-only point cloud, reducing gaps and blind spots while increasing the point cloud's volumetric density. It provides a more comprehensive multi-perspective representation of the rock slope. The results highlight the effectiveness of multi-source 3D point clouds fusion in complex geological settings, particularly in regions characterized by highly variable topography and geomorphology. And the multi-source 3D point clouds serve as a robust foundation for accurately identifying and extracting rockmass structural parameters. Intelligent algorithms then applied to this data identified more than 290 joints within the representative area using DSE software (Riquelme et al., 2015). A 3D model with colour rendered point cloud data (Figure 5) facilitated further analysis.

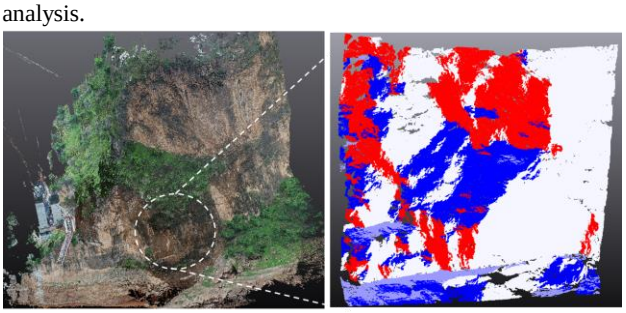

Figure 5. Multi-source 3D point clouds fusion from TLS-UAV technologies, joint identification results of the representative area and the same color band represents joint sets with similar orientations.

4.3 Rock hazard index (*RHI*)

A comprehensive statistical analysis was conducted to characterize the key geometric properties of rock joints within the representative area in the high and steep rock slope, focusing on four critical parameters: orientation, joint surface characteristic persistence distribution, and spacing distribution (Liu et al., 2025). As shown in Figure 6 and Table 2, the stability of hazardous rock masses in this area is primarily influenced and controlled by four distinct sets of joints. Among them, J1 is the most developed and runs nearly parallel to the surface of the rock slope. The spacing of J1 varies considerably, with an average of 2.27 m. In contrast, the joint set J2 and J3 exhibit more consistent spacing, averaging 0.81 m and 0.82 m, respectively. J9-4 is the most densely distributed, with an average spacing of 0.50 m. Additionally, notable variations exist in the size and scale of the structural planes across different sets. The average trace lengths of the joint sets J1, J2, J3, and J4 are 1.09 m, 2.17 m, 1.68 m, and 1.73 m, respectively.

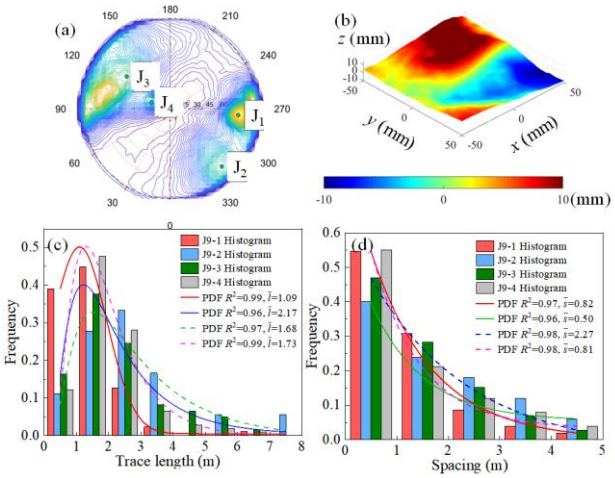

Figure 6. Statistical results of rock joint parameters within the representative area in the high and steep rock slope: (a) Stereographic projection of the joints at the representative area; (b) morphology characteristic of the representative dominant joint in the area; (c) histograms and probability density function (PDF) curves of joint trace length within the representative area; and (d) histograms and PDF curves of joint spacings within the representative area.

Joint set	Number	Mean orientation (°)	Mean persistence (m)	Mean spacing (m)
J1	75	274°∠81°	1.09	0.82
J2	108	320°∠82°	2.17	0.50
J3	79	110°∠62°	1.68	2.27
J4	29	284°∠15°	1.73	0.81

Table 2 Statistical results of orientation, persistence, and spacing of each joint set within the representative area in the high and steep rock slope.

The cohesion c and friction angle φ are key parameters in evaluating the shear strength of rock joints. Following the *M-JCS* model proposed by Liu et al. (2024a) (Equation 5), the shear strength of the joints under was calculated varying normal stress. Linear regression analysis was used to derive the shear strength parameters for the rock joints, with c ranging from 0 to 0.5 MPa and φ varying between 28° and 40°. The corresponding geometric parameters of the representative area were input into the *SMRTool* software (Riquelme et al., 2014). The spatial relationship between the rock joints and the slope surface was analyzed, leading to the determination of the slope quality grade.

$$\tau = \sigma_n \tan\left[(90.56M - 12.02)\lg\left(\frac{JCS}{\sigma_n}\right) + 0.414N + 9.273\right] \quad (5)$$

A rock hazard index (*RHI*) was developed, integrating joint geometric features (*JGF)*, joint mechanical features (*JMF*), and slope quality grade (*SMR*), to quantify risk levels (Liu et al., 2025). The risk of instability in hazardous rock masses increases with the trace length l and slope quality grade *SMR*, while it decreases with the spacing s and shear strength parameters (c, φ). To address discrepancies caused by varying data types, the parameters l, s, c, φ, and *SMR* were subjected to min-max normalization (Equation 6). This process produced normalized parameters—*JGFl*, *JGFs*, *JMFc*, *JMFφ* and *SMR*—ranging from 0 to 1.

$$RHI = JGFl + JGFs + JMFc + JMF\varphi + SMR \quad (6)$$

where *JGFl*, *JGFs*, *JMFc*, *JMFφ*, and *SMR* represent the normalized trace length, spacing, cohesion, friction angle of joints, and slope mass rating, respectively.

After calculating the parameters for each joint set in the representative area using Equation (6), the instability risk of the rock mass was evaluated based on the most critical combination of parameters. The joint set with the highest risk was selected, with the following values: *JGFl* = 0.43, *JGFs* = 0.83, *SMR* = 0.25, *JMFc* = 0.90, and *JMFφ* = 0.91. Using these values, the *RHI* value was determined to be 3.32 (Figure. 7). Consequently, the risk level of the representative area was categorized as high. Field investigations identified multiple rockfall scars in the area, confirming that the representative area is in a high-risk condition, which poses a considerable threat to road safety. This observation underscores the validity and effectiveness of the proposed research approach.

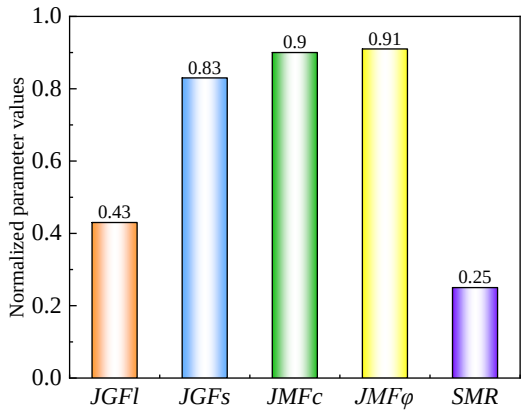

Figure 7. Summary of indicator scores and rock mass hazard index (*RHI*) assessment for the representative area in the high and steep rock slope.

5. Conclusion

This study underscores the significance of utilizing TLS-UAV technologies to evaluate the risk of rockmass hazard sources. The results provide valuable insights for the safe construction of major transportation projects and disaster prevention in mountainous areas. The key findings are as follows:

1. A multi-source data fusion methodology was developed, combining TLS and UAV-derived point clouds to achieve 19% improvement in spatial coverage and point cloud density compared to single-source modeling approaches, enabling comprehensive slope characterization.

2. Rock joins were intelligently identified within the multi-source 3D point clouds, allowing for precise delineation of rock dominant joint sets and extraction of spatial geometric information such as persistence, spacing, and roughness.

3. A rock hazard index (*RHI*) was developed, integrating joint geometric features (*JGF)*, joint mechanical features (*JMF*), and slope quality grade (*SMR*), to quantify risk levels of rockmass hazard sources within the multi-source 3D point clouds. The representative area was identified as the high-risk level, requiring immediate mitigation.

Acknowledgements

This work is supported by the JSPS Kakenhi (Grants-in-Aid for Scientific Research 23K13419), the Co-Creation Center for Disaster Resilience, Tohoku University and the Cross-Ministerial Strategic Innovation Promotion Program (Grant Number JPJ012289), and the National Natural Science Foundation of China (Grant Nos.42177142 and 41941019).

References

An L, Zhou P, Zhou M, et al., 2024: PointTr: Low-Overlap Point Cloud Registration with Transformer. *IEEE Sensors Journal*. doi.org/10.1109/JSEN.2024.3371021

Battulwar, R., Zare-Naghadehi, M., Emami, E., Sattarvand, J., 2021: A state-of-the-art review of automated extraction of rock mass discontinuity characteristics using three-dimensional surface models. *J. Rock Mech. Geotech. Eng.*, 13, 920–936. doi.org/10.1016/j.jrmge.2021.01.008.

Besl, P.J., McKay, N.D., 1992: A method for registration of 3-D shapes. *IEEE Trans. Pattern Anal. Mach. Intell.*, 14, 239–256. doi.org/10.1109/34.121791.

Ge, Y., Chen, Q., Tang, H., Cao, B., Hussain, W., 2023: A Semi-automatic Approach to Quantifying the Geological Strength Index Using Terrestrial Laser Scanning. *Rock Mech. Rock Eng.*, 56, 6559–6579, doi.org/10.1007/s00603-023-03412-1.

Herrero, M.J., Pérez-Fortes, A.P., Escavy, J.I., Insua-Arévalo, J.M., De la Horra, R., López-Acevedo, F., Trigos, L., 2022: 3D model generated from UAV photogrammetry and semi-automated rock mass characterization. *Comput. Geosci.*, 163. doi.org/10.1016/j.cageo.2022.105121.

Huang S, Gojcic Z, Usvyatsov M, et al., 2021: Predator: Registration of 3d point clouds with low overlap. *Proceedings of the IEEE/CVF Conference on computer vision and pattern recognition*. 4267-4276.

Kong, D., Saroglou, C., Wu, F., Sha, P., Li, B., 2021: Development and application of UAV-SfM photogrammetry for quantitative characterization of rock mass discontinuities. *Int. J. Rock Mech. Min. Sci.*, 141, doi.org/10.1016/j.ijrmms.2021.104729.

Lan, H., Zhang, Y., Macciotta, R., Li, L., Wu, Y., Bao, H., Peng, J., 2022: The role of discontinuities in the susceptibility, development, and runout of rock avalanches: a review. *Landslides*, 19, 1391–1404. doi.org/10.1007/s10346-022-01868-w.

Lan, H., Zhao, Z., Li, L., et al., 2024: Climate change drives flooding risk increases in the Yellow River Basin. *Geography and Sustainability*, 5(2), 193–199, doi.org/10.1016/j.geosus.2024.01.004.

Li, B., Gong, W., Tang, H., Wang, L., 2024: DEM simulation of the bridge collapse under the impact of rock avalanche: a case study of the 2020 Yaoheba rock avalanche in Southwest

China. *Bull. Eng. Geol. Environ.*, 83. doi.org/10.1007/s10064-024-03604-1.

Li, H.B., Li, X.W., Li, W.Z., Zhang, S.L., Zhou, J.W., 2019: Quantitative assessment for the rockfall hazard in a post-earthquake high rock slope using terrestrial laser scanning. *Eng. Geol.*, 248, 1–13. doi.org/10.1016/j.enggeo.2018.11.003.

Li, Y., Chen, J., Zhou, F., Bao, Y., Li, Z., Song, S., Cao, C., 2022: Stability evaluation of rock slope based on discrete fracture network and discrete element model: a case study for the right bank of Yigong Zangbu Bridge. *Acta Geotech.*, 17, 1423–1441, doi.org/10.1007/s11440-021-01369-5.

Liu, C.Q., Bao, H., Lan, H.X., Yan, C.G., Li, C.B., Liu, S.J., 2024a: Failure evaluation and control factor analysis of slope block instability along traffic corridor in Southeastern Tibet. *J. Mt. Sci.*, 21, 1830–1848. doi.org/10.1007/s11629-023-8484-9.

Liu, C.Q., Bao, H., Lan, H.X., Li, L., Chen, W.C., Lv, H.T., Liu, J.H., Liu, S.J., 2024b: Bedding effect on progressive crack propagation in layered sandstone grotto roof. Tunn. Undergr. Space Technol. 152, 105914. doi.org/10.1016/j.tust.2024.105914.

Liu, C.Q., Bao, H., Wang, T., et al., 2025: Intelligent characterization of discontinuities and heterogeneity evaluation of potential hazard sources in high-steep rock slope by TLS-UAV technology. J. Rock Mech. Geotech. Eng. doi.org/10.1016/j.jrmge.2025.03.023.

Loiotine, L., Andriani, G.F., Jaboyedoff, M., Parise, M., Derron, M.-H., 2021: Comparison of remote sensing techniques for geostructural analysis and cliff monitoring in coastal areas of high tourist attraction: The case study of Polignano a Mare (southern Italy). *Remote Sens.*, 13, doi.org/10.3390/rs13245045.

Mao, Z., Hu, S., Wang, N., et al., 2021: Precision evaluation and fusion of topographic data based on UAVs and TLS surveys of a loess landslide. *Front. Earth Sci.*, 9, 801293. doi.org/10.3389/feart.2021.801293.

Marani, R., Renò, V., Nitti, M., D’Orazio, T., Stella, E., 2016: A Modified Iterative Closest Point Algorithm for 3D Point Cloud Registration. *Comput.-Aided Civ. Infrastruct. Eng.*, 31, 515–534, doi.org/10.1111/mice.12184.

Martínez-Carricondo, P., Agüera-Vega, F., Carvajal-Ramírez, F., Mesas-Carrascosa, F.-J., García-Ferrer, A., Pérez-Porras, F.-J., 2018: Assessment of UAV-photogrammetric mapping accuracy based on variation of ground control points. *Int. J. Appl. Earth Obs.*, 72, 1–10, doi.org/10.1016/j.jag.2018.05.015.

Mirhadi, N., Macciotta, R., 2023: Quantitative correlation between rock fall and weather seasonality to predict changes in rock fall hazard with climate change. *Landslides*, 20, 2227–2241. doi.org/10.1007/s10346-023-02105-8.

Riquelme, A.J., Abellán, A., Tomás, R., 2015: Discontinuity spacing analysis in rock masses using 3D point clouds. *Eng. Geol.*, 195, 185–195. doi.org/10.1016/j.enggeo.2015.06.009.

Riquelme, A.J., Abellán, A., Tomás, R., Jaboyedoff, M., 2014: A new approach for semi-automatic rock mass joints recognition from 3D point clouds. *Comput. Geosci.*, 68, 38–52. doi.org/10.1016/j.cageo.2014.03.014.

Shan, Q., Wu, C., Curless, B., et al., 2014: Accurate geo-registration by ground-to-aerial image matching. *Proc. 2nd Int. Conf. 3D Vision*, IEEE, 1, 525–532. doi.org/10.1109/3DV.2014.69.

Xu, X., Bao, H., Lan, H., Liu, C., Xu, J., Yan, C., 2022: Sampling interval-size effects and differential sensitivities of different morphology parameters of rock joint. *J. Struct. Geol.*, 155. doi.org/10.1016/j.jsg.2022.104530.

Yuan, W., Ran, W., Shi, X., Shibasaki, R., 2023: Multi-Constraint Transformer based Automatic Building Extraction from High Resolution Remote Sensing Images. *IEEE J. Sel. Top. Appl. Earth Obs. Remote Sens.*, 16, 9164–9174. doi.org/10.1109/JSTARS.2023.3319826.

Yuan, W., Yuan, X., Cai, Y., Shibasaki, R., 2023: Fully automatic DOM generation method based on optical flow field dense image matching. *Geo-Spatial Inf. Sci.*, 26(2), 242–256. doi.org/10.1080/10095020.2022.2159886.

Zang, Y., Yang, B., Li, J., et al., 2019: An accurate TLS and UAV image point clouds registration method for deformation detection of chaotic hillside areas. *Remote Sens.*, 11(6), 647. doi.org/10.3390/rs11060647.

Zhao, S., Dai, F., Deng, J., Wen, H., Li, H., Chen, F., 2023: Insights into landslide development and susceptibility in extremely complex alpine geoenvironments along the western Sichuan–Tibet Engineering Corridor, China. *Catena*, 227. doi.org/10.1016/j.catena.2023.107105.

Zhao, S., Dai, F., Deng, J., Wen, H., Li, H., Chen, F., 2023: Insights into landslide development and susceptibility in extremely complex alpine geoenvironments along the western Sichuan–Tibet Engineering Corridor, China. *Catena*, 227. doi.org/10.1016/j.catena.2023.107105.